Reference: *Biol. Bull.* **227:** 40–50. (August 2014)

A Nose Too Far: Regional Differences in Olfactory Receptor Neuron Efficacy Along the Crayfish Antennule

DEFOREST MELLON, JR.[1,*], SWAPNIL PRAVIN[2] AND MATTHEW A. REIDENBACH[3]

[1]*Department of Biology, University of Virginia, Charlottesville, Virginia 22904;* [2]*Department of Mechanical and Aerospace Engineering, University of Virginia, Charlottesville, Virginia 22904; and* [3]*Department of Environmental Sciences, University of Virginia, Charlottesville, Virginia 22904*

Abstract. The olfactory sense organs of crayfish are aesthetasc sensilla, arrayed along the distal half of the lateral antennular flagella on each side of the animal. The sensillar array is sparse at its proximal origin, where each annulus houses only a single aesthetasc, and it is most dense distally, with occasionally up to six aesthetascs residing on each antennular annulus. Previous studies have tacitly assumed that the aesthetascs are co-equal in their functional properties. We restricted exposure of small zones of aesthetascs to odorant along the array, from near its proximal origin, its midpoint, and its termination near the tip of the lateral flagellum, while recording neural responses within the ipsilateral olfactory lobe of the brain. Simultaneous combinations of zonal exposure to odorant gave proportionally larger central responses, indicative of spatial summation of peripheral inputs. Surprisingly, however, zonal effectiveness was not equal; stimulating even small numbers of aesthetascs near the proximal origin of the array was far more excitatory to local deutocerebral interneurons than stimulating greater numbers of aesthetascs at the tip of the flagellum. The results are discussed in terms of continuing growth and attrition of the antennular segmentation and associated olfactory receptor neurons.

Introduction

Capture of odorant stimuli by olfactory receptors in both vertebrates and invertebrates has received increasing attention since the initial cloning of mammalian genes expressing odorant receptor proteins in the early 1990s. The presence and distribution of receptor proteins on olfactory receptor neurons (ORNs) is well documented (Buck and Axel, 1991; Ressler *et al.,* 1993; Zhang and Firestein, 2002; Elmore *et al.,* 2003; Goldman *et al.,* 2005), and the patterns of central targeting by ORN axons have been successfully examined in both mammals and insects, where molecular genetic techniques have been especially compelling in demonstrating the specificity of anatomical relationships between identified olfactory glomeruli and the various ORN classes (Mombaerts *et al.,* 1996; Dynes and Ngai, 1998; Vosshal *et al.,* 1999, 2000; Zou *et al.,* 2001; Hallem *et al.,* 2004). Other studies have focused upon the molecular structure of olfactory stimuli and, especially, the nature of signal transduction pathways leading to the generation of ORN spiking activity (Boehkoff *et al.,* 1994; Zufall *et al.,* 1994; Hildebrand and Shepherd, 1997).

Much less is understood, however, about the numerical and functional relationships between ORNs and their individual target brain neurons. What are the biological constraints that dictate the most effective ratio of ORNs to their central neuronal targets? Does conjoint stimulation of individual ORNs by an odorant enhance the response of target brain neurons through simple summation, or is there nonlinearity as the stimulated fraction of the homologous receptor array by the odorant increases? Finally, are all competent ORNs within the sensilla array equivalent in their individual responses to the same odorant? These and other questions related to the physical disposition and physiological relationships of ORNs on all metazoan sensory structures remain poorly understood.

Received 13 December 2013; accepted 22 March 2014.

* To whom correspondence should be addressed. E-mail: dm6d @virginia.edu

Abbreviations: OL, olfactory lobe; ORN, olfactory receptor neuron; PLIF, planar lasar-induced fluorescence.

In crustaceans, olfactory sensilla, referred to as aesthetascs, occur on the lateral flagellum of each antennule (Sandeman and Denberg, 1976; Tierney *et al.,* 1986; Grünert and Ache, 1988; Mellon *et al.,* 1989), and each aesthetasc houses the distal dendrites of a variable number, usually 100–300, of olfactory receptor neurons (ORNs). Aesthetasc assemblages in many, if not most, crustaceans occur in comparatively short, dense tufts. This is the case with marine species such as palinurids, homarids, anomurids, and the brachyura. In a few species, however, such as freshwater crayfishes and caridean prawns, the aesthetascs are rather sparsely arrayed linearly along the distal one half of the flagellum (Tierney *et al.,* 1986; Mellon *et al.,* 1989; Mellon and Munger, 1990; Hallberg *et al.,* 1992). The spatially distributed arrangement of aesthetasc sensilla in these animals provides an unusual opportunity to determine the extent to which fractional regions of the receptor array contribute to the central representation of odorants. Furthermore, crayfish antennular flagella grow continuously throughout an animal's lifespan by adding annuli and sensilla at their base; this means that aesthetascs near the flagellum tip are the oldest, and in adult individuals a proportion of them, along with the distal annuli, are shed at each molt (Sandeman and Sandeman, 1996). The linear distribution of sensilla, representing a spatial gradation in age, requires examination of possible age-related variations in odorant sensitivities of aesthetascs in different regions along the flagellar shaft. Moreover, because at least some local interneurons within the deutocerebrum receive short-latency inputs from hydrodynamic receptors on the antennular flagella in addition to long-latency inputs from the aesthetascs (Mellon, 2005), interactions between the different central response phases may depend critically upon the transmission time to the brain from the receptor neurons in the different regions of the lateral flagellum. To address questions of spatial summation within the aesthetasc array and competency of ORNs along the array, we designed an olfactometer to effect regional stimulation of the aesthetasc array while recording electrical activity from olfactory lobe (OL) interneurons in the brain of the crayfish *Procambarus clarkii* Girard. This apparatus permitted separate or conjoint stimulation by odorant at three different zones along the aesthetasc array: near the antennular flagellum tip (zone 3), in the middle of the array (zone 2), and just distal to the proximal origin of the array (zone 1), roughly halfway between the flagellum base and the tip. We examined the responses of Type I local deutocerebral interneurons—broad-spectrum multiglomerular cells first characterized by Mellon and Alones (1995) and which are driven by excitatory synaptic input from ipsilateral olfactory receptor neurons associated with the aesthetascs on the antennules—from 22 preparations to stimulation of different numbers of aesthetascs, including 14 cells from which we were able to determine a detailed differential response to zonal stimulation. The results of our studies permit us to conclude that odorant stimulation of a larger fraction of the sensilla array generally produces larger responses in OL neurons than smaller fractional stimulation. Furthermore, proximally positioned aesthetascs generate dramatically more vigorous responses within the Type I neurons than those located at the middle or distal regions of the array. The stimulation techniques were verified both by using an active computer model of stimulus flow to examine the accuracy of the stimulus operation as well as by directly observing the stimulant flows' restrictions exclusively to the three respective zones on the flagellum by means of planar laser-induced fluorescence (PLIF).

Materials and Methods

Animals used were large adult (50–60-mm carapace length) individuals of the southern red swamp crayfish *Procambarus clarkii* having antennules at least 25 mm in length. Crayfish were de-clawed and maintained in pairs in individual plastic tubs having about 3 cm of dechlorinated tap water, at room temperatures. Water was changed every other day. The crayfish were fed on frog chow and lettuce twice a week.

For electrophysiological experiments, crayfish were chilled in crushed ice for about 30 min to anesthetize them. They were then decapitated by transverse cutting through the cephalothorax at a level just caudal to the base of the rostrum. The head capsule was rinsed in chilled crayfish saline (composition in mmol l^{-1}: NaCl, 205; KCl, 5.4; $CaCl_2 \cdot 2H_2O$, 13.6; $MCl_2 \cdot 7H_2O$, 2.7; $NaHCO_3$, 2.4; and the pH adjusted to 7.4 with HCl), and the rostrum was removed. The isolated heads were mounted in a recording chamber, as described previously (Mellon, 2005), except that all four antennular flagella were drawn by suction into the olfactometer diagrammed in Figure 1 through a small opening in an acrylic plastic partition. This provided a modicum of mechanical and, hence, positional stability to the flexible antennular flagella within the central channel of the olfactometer. Animals having discolored or broken aesthetascs were not used in this study. The olfactometer consisted of a central cylindrical channel, 25 mm in length and 1.2 mm in diameter, that was aligned with the opening in the recording chamber and open at the opposite end. The bases of the antennules were sealed within the olfactometer with petroleum jelly to isolate them from the recording chamber.

Three pairs of transversely aligned side channels, 1.1 mm in diameter, intersected the main channel at, respectively, 2.5 mm, 7.5 mm, and 12 mm from the distal opening of the main olfactometer channel, as shown in Figure 1B. On the top of the olfactometer near the recording chamber, a vertical cylindrical channel 1.2 mm in diameter intersected the main channel from above. The vertical channel provided access to a reservoir of dechlorinated tap water, which

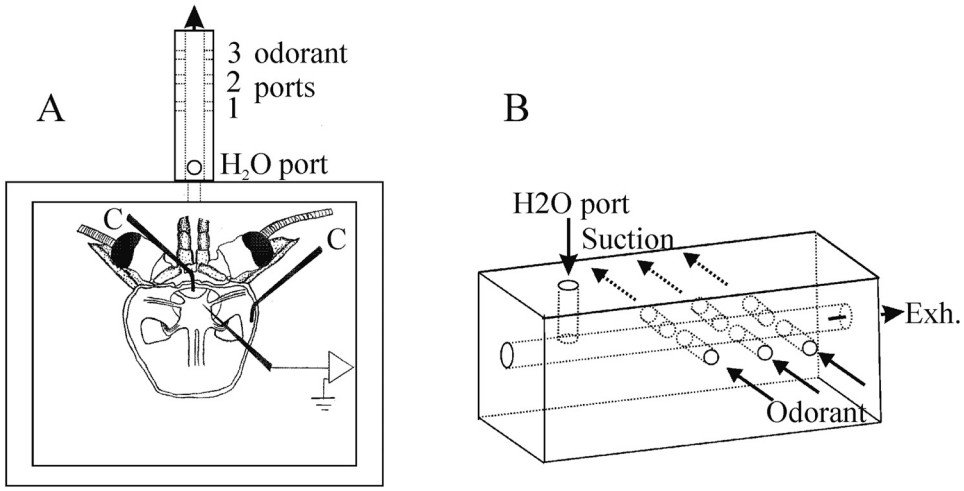

Figure 1. (A) Diagram of the isolated head preparation and partitioned olfactometer used in the experimental procedures. The antennular flagella protrude through an aperture in the wall of the square recording chamber and into the olfactometer. Cannulas for brain perfusion and the recoding electrode placement are labeled "C." (B) Detail of the partitioned olfactometer. Antennular flagella (not shown) protrude into the central horizontal chamber from the left and extend to the right beyond the most distal odorant port. Water enters the olfactometer chamber through the vertical port, while odorant enters through the three horizontal ports labeled "Odorant" and is removed *via* the ports labeled "Suction" after passing across the flagella.

exited by gravity flow through the distal opening into a sump after flowing past the antennular flagella. The maximal flow rate of water through the central chamber when it was occupied by the four antennular flagella was 15.6 ml/min. Each of the three side channels on one side could be individually connected by an electronically controlled solenoid switch to an odorant reservoir containing 0.05% tetramin solution, made up by dissolving 1 g of Tetramin fish food pellets in 100 ml of dechlorinated tap water and diluting appropriately. The same electrical pulses used to control odorant access also opened the paired, opposite side channels to a vacuum source, so that, during stimulation from a port, odorant *and reservoir water* were drawn across the main channel, past the antennular flagella, and into the vacuum exhaust channel. Protocol for water and stimulus delivery at each zone were as follows: (1) water onset; (2) odorant onset 2 s later for 0.5 s; (3) water off 8 s later.

As soon as the isolated head had been mounted in the recording chamber, the median (cerebral) artery and the lateral cephalic artery on one side of the head were cannulated and perfused with chilled (16° C) oxygenated crayfish saline at a flow rate of 2 ml/min. The perineurium was removed from the dorsal surface of the brain to expose the OLs. Sharp micropipette electrodes filled with 2 mol l^{-1} potassium acetate were used to impale the large dendritic trunks of Type I local interneurons within the OL. Type I interneurons are the largest neurons that have been characterized in the crayfish deutocerebrum (Mellon and Alones, 1995); with dendritic processes up to 20 μm in diameter within the OL, they can be more readily penetrated with sharp micropipette electrodes than any other resident interneurons. Signals from impaled neurons were led to an Axoclamp 2B amplifier (Molecular Devices, Sunnyvale, CA), digitized, and stored in a computer file for later analysis. Solenoid switches (Lee Company, Westbrook, CT) used to deliver water and the odorant pulses and to control access to suction to the three stimulus ports were activated by Grass S48 stimulators (AstroMed, Warwick, RI) that could be energized separately, sequentially, or simultaneously. Odorant delivery was gravity-fed at 11 ml/min. Responses to odorant pulses were recorded as the number of spikes during a 5-s time window commencing 200 ms after odorant pulse onset (to avoid secondary hydrodynamic responses to fluid onset). Within each test series, sequential stimulation of specific ports or port combinations were varied randomly to obviate any possible effects of physiological deterioration of the preparation. Mean values for spike numbers in response to 2–13 repetitions—at 2-min intervals—of odorant pulses were computed and were divided by the number of aesthetasc sensilla within the stimulus column (= diameter of the stimulus port) at each zone to generate a response coefficient for that zone. In two preparations, only two or three observations in each of the seven stimulating situations were collected due to the loss of microelectrode penetration.

After response sequences were obtained from a preparation, the isolated head was left in place in the recording chamber, and the margins of the three stimulating zones within the aesthetasc array along the antennular flagellum were carefully measured, in terms of the identity of included flagellar annuli, using a dissecting microscope. The measurements were then translated to their fractional positions

(as percentage of the linear distance between the proximal origin of the aesthetasc array and its termination at the flagellar tip) along a dimensionless variable axis *(z)* representing the array of aesthetascs; essentially, the respective lengths of the aesthetasc arrays in different animals were normalized, 0 to 1. Finally, the number of aesthetascs within the boundaries of the identified annuli in each of the three stimulus zones was carefully counted and recorded using a compound microscope.

The absence of odorant spread between the three stimulus ports lengthwise along the water channel was verified by visualizing the flow of odorant across the central channel from each of the supply ports to the corresponding suction-exhaust port. Planar laser induced fluorescence (PLIF) was thereby used to verify that odorant flow through each of the pairs of side channels was confined to that pair of channels alone during actual tests with antennules from moribund crayfish heads identical in size to those used in the experiments with living material. This technique used fluorescein dye (molecular diffusion in water, $D = 0.5 \times 10^{-9}$ m^2 s^{-1}) as the scalar tracer, while a 488-nm laser was used to excite the fluorescein (mean excitation at 490 nm and mean emission at 520 nm). The laser beam was first passed through a beam focus and then aligned to illuminate only the antennule chamber by directing the laser beam into the exhaust port of the chamber. Fluorescein dye was added independently into each of the three stimulus ports and injected into the main chamber. A digital camera (1 Mpixel, 12-bit resolution) (Dalsa 1M60, Waterloo, Ontario, Canada) imaged the fluoresced light through the top of the chamber, which was optically transparent. The camera was fitted with a longpass filter, which passed all light above 517 nm from the excited dye, while ambient laser light was blocked. Light intensity emitted from the fluorescein dye is directly proportional to dye concentration, and a linear correlation between light emission and dye concentration was formed. The aperture of the camera was adjusted such that the source concentration of the dye injected into the chamber corresponded to near-saturation levels of light into the camera. Since the camera has 12-bit resolution, concentrations could be quantified down to 1/4096 of the source concentration. Figure 2 shows the colormap of dye concentration within the chamber during separate, sequential dye releases within each port, which closely matches the numerical simulation. This figure also shows that dye does not escape out of the exhaust port of the chamber.

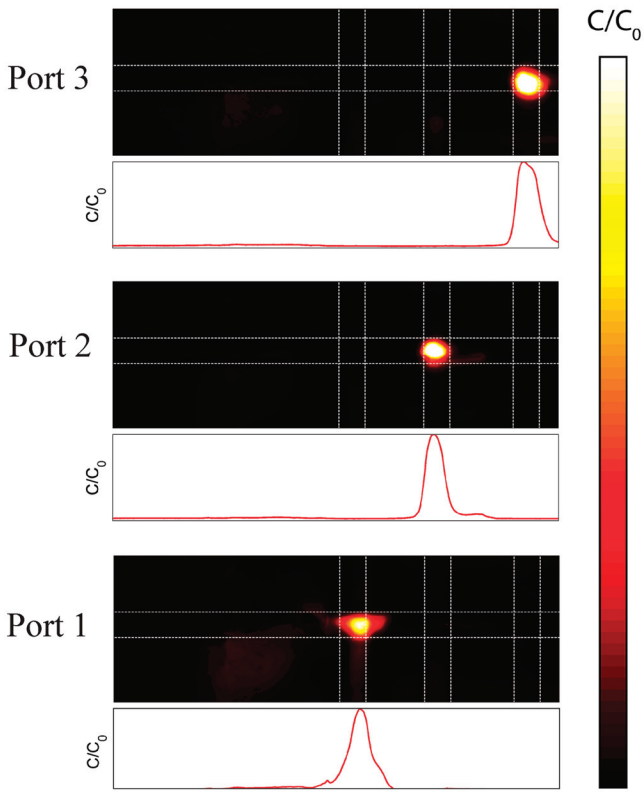

Figure 2. Planar laser-induced fluorescence images of dye within the central cylindrical chamber (denoted by dashed horizontal lines) where the antennule is located, sequentially applied through each of the three transversely aligned side channels (denoted by the dashed vertical lines). Concentration is normalized by input concentration and shows little mixing within the central chamber.

Results

Antennular anatomy and aesthetasc distribution

Figure 3A is a phase contrast light micrograph of a portion of a living lateral flagellum from *Procambarus clarkii.* Aesthetasc sensilla (white arrows) are blunt setae roughly 100-μm long, 10–15 μm in diameter at their base and tapering to a smaller diameter at their tip. The distal 40% of each aesthetasc has a thin (1-μm thick) optically transparent cuticle that is apparently the region through which odorant molecules can pass to the interior (Tierney *et al.,* 1986). Each aesthetasc houses the distal dendrites of approximately 175 ORNs (Mellon *et al.,* 1989); within the distal reaches of each aesthetasc the distal dendrites individually branch repeatedly into single microtubules, in which are imbedded olfactory receptor proteins. It is not known whether the number of ORNs associated with aesthetascs at different locations within the linear array is variable, nor if the number of functionally viable ORNs varies with the age of the aesthetascs.

In the crayfish, aesthetasc sensilla are arrayed along the ventral aspect of the distal one-half of the lateral antennular flagellum. Their axial density along the array varies dramatically from the origin of the array to its termination near the tip of the flagellum, with low densities at the origin compared to those at the tip. The differences in aesthetasc density can be appreciated from the light micrographs of regions of a lateral flagellum, freshly excised from a large adult *P. clarkii,* in Figure 3B–D, showing sample annuli

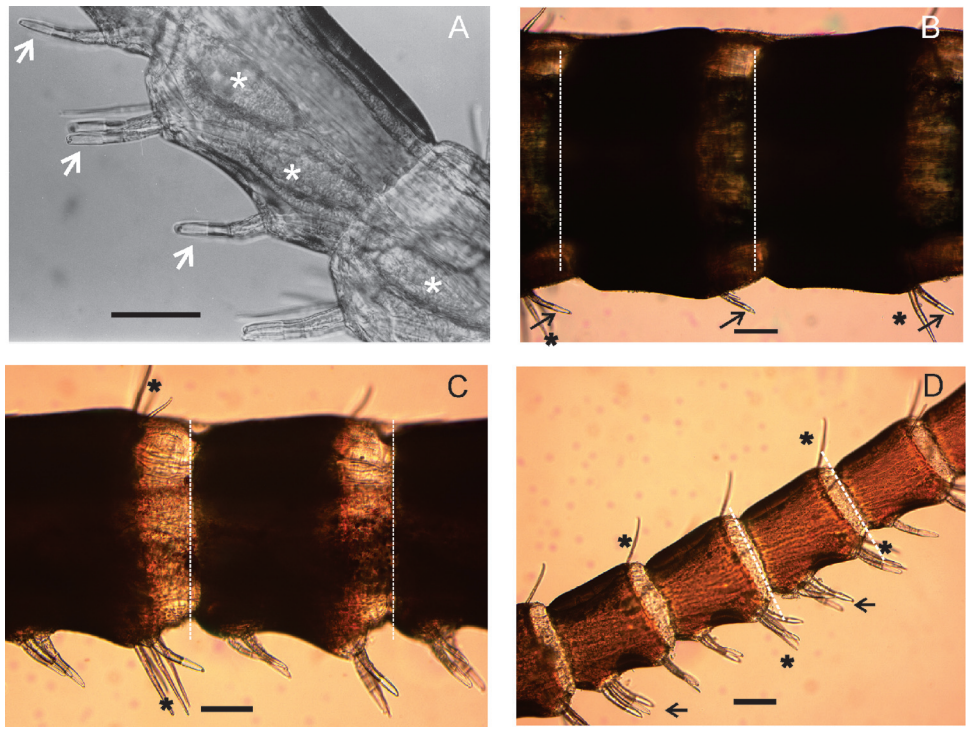

Figure 3. (A) Phase contrast micrograph of portion of a living lateral antennular flagellum from *Procambarus clarkii,* modified from Mellon *et al.* (1989). Aesthetasc sensilla are indicated by white arrows; each aesthetasc is supplied by the distal dendritic segments from approximately 175 olfactory receptor neurons, the cell bodies of which are clustered in individual sensory ganglia that are partially visible (asterisks) through the flagellar cuticle. (B) Light micrograph of a portion of a freshly excised lateral antennular flagellum from *P. clarkii*. The two antennular annuli included in the image (annulus borders indicated by white dashed lines) are from a region just distal to the origin of the aesthetasc array; each annulus in this region generally bears just a single aesthetasc (black arrows). Additional, numerous setae seen in micrographs B–D (black asterisks) are beaked sensilla (Mellon, 2012) believed to serve a bimodal mechano-chemosensory function). (C) Micrograph from the same lateral flagellum as in B, but from a region about 40% of the total length of the array distal to the origin ($z \sim 0.4$). Here, each annulus is smaller than those near the array origin, and each bears three to four aesthetasc sensilla. (D) A portion of the same flagellum near the tip; aesthetascs often occur in clusters of three (arrows) at the proximal edge of an annulus and two at the distal edge, for a total of four to five per annulus, each of which is only about one-third the size of those shown in C and which, therefore, present greater numbers of aesthetascs exposed to the odorant stimuli at the port. All scale bars are 100 μm.

from (B) the region near the origin of the aesthetasc array, (C) a region close to the center of the array, and (D) a region just proximal to the tip of the flagellum, the distal termination of the array. At the array's origin, aesthetasc density per annulus varies from 1 per annulus (or 1 every other annulus) to 2 per annulus. In the center of the array the density is usually 3–4 per annulus, whereas near the tip the density is 4–5 per annulus. These changes are graphically illustrated in Figure 4, showing the aesthetasc distribution along the array, proximal-to-distal, in four lateral flagella taken from three different animals of about 55 mm in carapace length. The array is usually about 13–15 mm in length in crayfish of this size, but here in each case the array has been converted to a dimensionless variable, *Z,* that varies between 0 (at the origin) and 1 (at the tip). The vertical rectangles in Figure 4A, labeled 1–3, indicate the approximate extent and position of the stimulus ports within a typical aesthetasc array.

Neurophysiological observations

Initial studies with several perfused isolated head preparations were designed to examine the role of individual groups of aesthetascs regardless of their position along the lateral flagellum array. Experiments were performed using the olfactometer illustrated in Figure 1, having three approximately equally spaced odorant ports operated separately or in different simultaneous combinations to stimulate the aesthetasc zones, that is, zones 1, 2, 3, 1+2, 1+3, 2+3, or 1+2+3. As described above and graphically in Figure 4, in an adult individual of *P. clarkii*, the density of aesthetascs

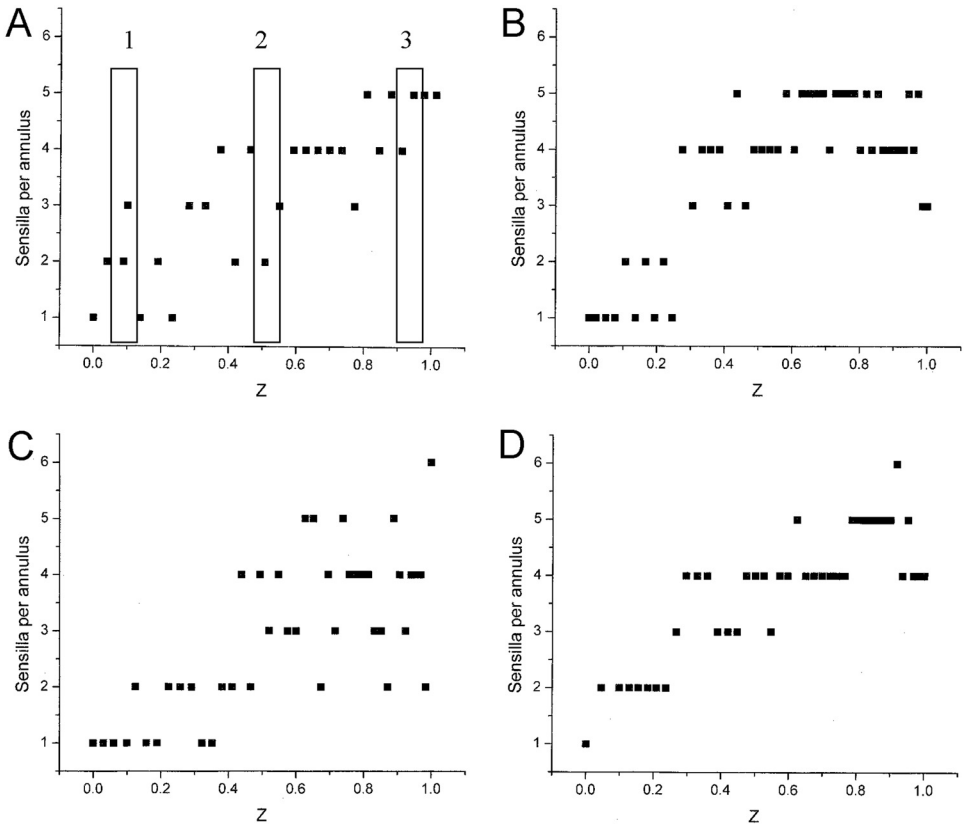

Figure 4. Distribution of aesthetasc number per annulus along the array in four freshly excised lateral antennular flagella from animals in the range of 55–60-mm carapace length. (A and B) are from opposite sides of the same crayfish; (C and D) are from two different crayfish. The sensilla arrays, occupying between 32 and 42 flagellar annuli, are represented as dimensionless variables, *z*, where 0 is at the origin of the array, roughly halfway distal from the base of the flagellum, and 1 is the termination of the array at the tip. The vertical rectangles in A approximate the position of ports 1, 2, and 3 with respect to the aesthetasc array. While there is considerable variability between individual flagella, it is clear that the most proximal annuli harbor the fewest aesthetascs and that the density of aesthetascs per annulus increases distally.

per antennular segment (annulus) varies from 0.5–2.0 near the proximal origin of the array to 4–6 near the distal termination of the array. The electrophysiological results from one isolated head preparation are shown in the records of Figure 5. They show spiking responses from a Type I neuron to 0.5-s applications of tetramin to zone 3 in A, zone 2 in B, zone 1 in C, and various combinations of zonal stimulus delivery in D–G. The concentration of odorant stimulus, its timing following water onset, and its duration were identical in A–C, although the spike number and mean frequency varied depending upon the stimulation zone. Surprisingly, the smallest response occurred to stimulation of port 3, an area of the flagellum where the density of aesthetasc sensilla is at its greatest; and the highest response was obtained following stimulation via port 1, where the aesthetasc density is very low. The results do show, however, that increasing the number of ports through which odorant was simultaneously applied increased the spiking response significantly: the response in D was obtained to simultaneous exposure of zones 2 and 3, that in E to exposure of zones 1 and 3, in F to simultaneous exposure of zones 1 and 2, and in G to exposure of all three ports together.

Data from three different preparations are shown in Figure 6; they are graphed together and illustrate the typical relationship between the response magnitude and the number of aesthetascs simultaneously stimulated. The relationship is highly statistically significant. Results from an additional five preparations are shown in Table 1. The mean spiking responses from each preparation are based upon from 2 to 13 measurements in each of the seven stimulus conditions described above, in which the number of aesthetascs exposed in each condition was counted. Regression analysis was used to analyze the relationships in Table 1; only the data from 5/24/12 were not statistically significant at the 0.05 probability level or less. Both Figure 6 and Table 1 indicate that the responses from each Type I cell in the brain are additive and depend upon the net increment in the

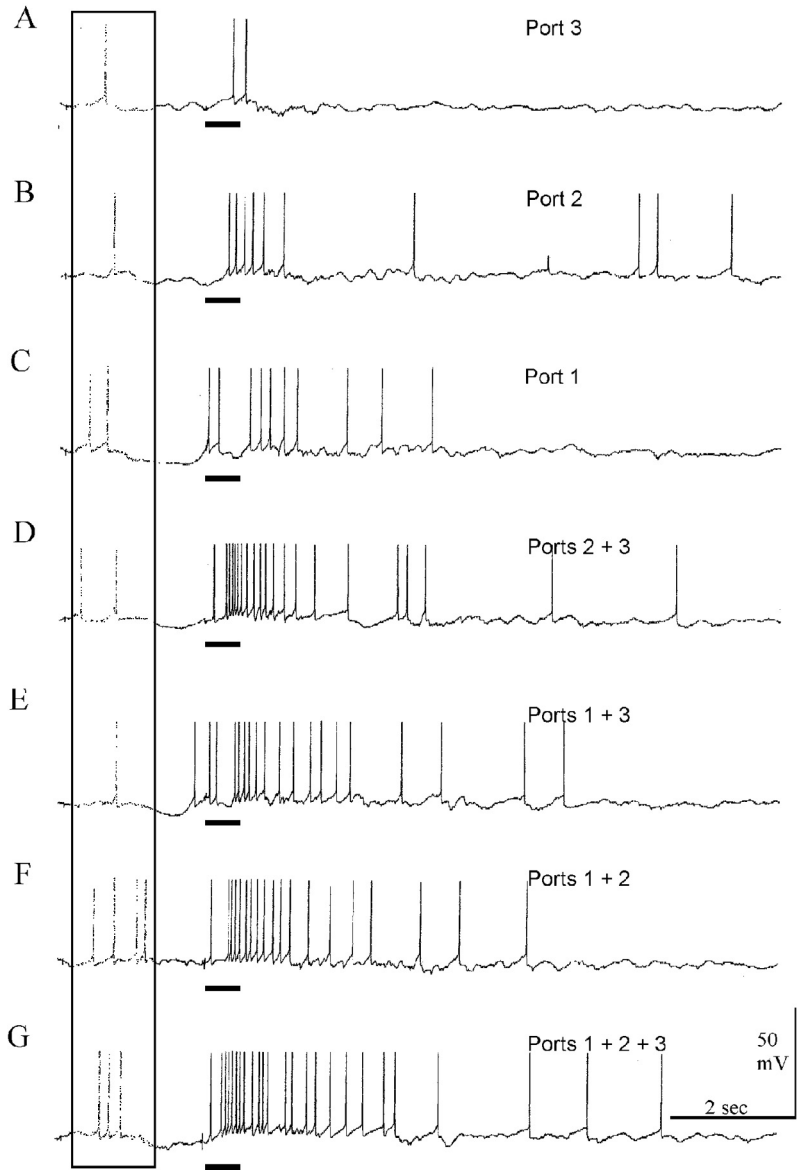

Figure 5. Electrical records from a Type I neuron exemplifying responses to zonal exposure of the lateral flagellum to odorant. (A–G) Responses to 0.5-s odorant pulses (solid bars beneath electrical records) *via* the indicated ports or port combinations, occurring 2 s after the onset of water through the central olfactometer chamber). The rectangle at the left delineates initial spikes generated by hydrodynamic inputs from the flagellum at the onset of water flow (Mellon, 2005). The number of aesthetascs exposed to odorant at port 1 was 1, the number exposed at port 2 was 16, and the number exposed at port 3 was 17. The *z* position of the aesthetasc array at port 1 was 0; that is, it was at the initial annulus of the array. Comparing the records in D–G with those in A–C, there is a clear indication of the additive relationship between central response and the extent of peripheral stimulation.

number of aesthetascs simultaneously exposed to a standard odorant pulse. A detailed examination of these data also suggested, however, that there was considerable variance in the overall effectiveness of different zonal stimulus combinations, with larger aesthetasc numbers at the distal part of the flagellum being much less effective than similar or even lesser numbers of aesthetascs from the more proximal locations. The spiking data were therefore converted to response coefficients by dividing the mean spike numbers obtained from stimulation at each port by the number of aesthetasc sensilla exposed to odorant *via* that port.

The bar graphs in Figure 7A illustrate the disparities in response coefficients of the three zonal regions in the aesthetasc array. The data represent mean values obtained

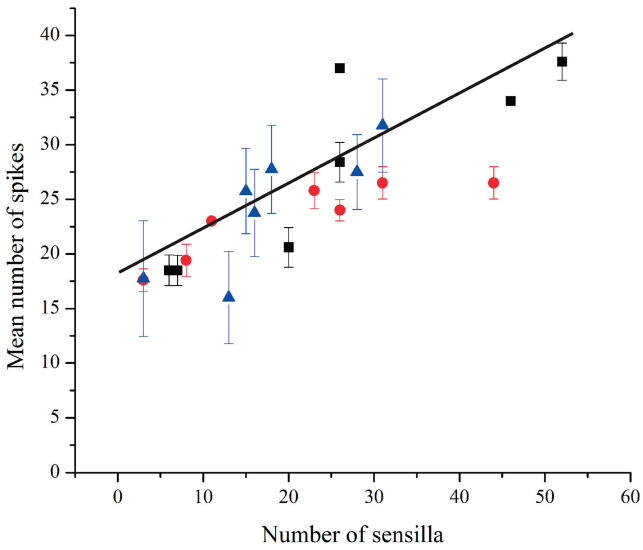

Figure 6. Spiking responses of three Type I interneurons to different numbers of stimulated aesthetascs, including those exposed by stimulus pulses in ports 1, 2, 3 and 1+2, 1+3, 2+3, and 1+2+3. The responses of individual Type I cells are indicated by the different colored symbols. The regression curve represents best linear fit of the combined data; it was calculated by least squares regression analysis and is represented by the equation $y = 0.41x + 18.57$. Pearson's r is 0.87 and $P > 0.0001$.

across 14 preparations. Even though they do not provide details of the disparities within individual flagella, they support the conclusion that aesthetascs near the proximal origin of the sensilla array are considerably more effective in exciting Type I cells within the OL than those located within the middle or tip regions of the array. This conclusion is strengthened by the graphic results displayed in Figure 7B, in which the response disparities in each of the same 14 preparations are shown with specific reference to relative spatial position of the stimulus zone within the aesthetasc array. Here, data are plotted as mean response coefficients against position along the aesthetasc array whose respective positions are represented as dimensionless variables between 0 and 1, with 0 as the proximal margin of the array and 1 being its termination at the tip of the flagellum. The position of each data point along the horizontal axis was taken as the midpoint of that group of aesthetascs centered within either ports 1, 2, or 3 and then converted to its fractional position, *Z,* within the array. It is clear from these data that stimulation of the proximal region of the array, near its origin, is considerably more effective in driving Type I neurons than stimulation at more distal regions.

Discussion

Our discussion of the experimental results begins with a brief review of the organization of the primary olfactory pathways in the crayfish, as currently understood. Within each aesthetasc, dendrites of the ganglionic olfactory receptor neurons (ORNs) divide into individual microtubules, and imbedded within the microtubular membrane are olfactory receptor proteins. By inference from the distribution of olfactory receptor associations in other animals (*e.g.,* rats, Mombaerts *et al.,* 1996; fruit flies, Vosshall *et al.,* 1999, 2000), there is a strong suggestion that the olfactory receptor proteins associated with each specific ORN type in a sensory ganglion are unique and bind unique classes of olfactory determinants on odorant molecules. Each aesthetasc, moreover, is thought to be a heterogeneous functional replica of its neighbors. Within the primary olfactory neuropil of the crayfish brain—the paired olfactory lobes (OLs)—it is thought that axon terminals of individual, class-specific ORNs from all of the antennular sensory ganglia are segregated each within their own, uniquely

Table 1

Spiking responses to stimulation by odorant in single zones and zonal combinations

	04/22/12(A)			04/22/12(B)			05/24/12			05/30/12			04/12/12		
Ports	Aes	APs	SE	Aes	APs	SE	Aes	APs	SE	Aes	APs	SE	Aes	APs	SE
1	14	9.7	0.7	14	6.2	0.86	1	10.5	1.95	8	17.6	0.71	7	18.5	1.97
2	17	8	0.01	17	4.6	0.51	16	11.3	1.5	11	10.1	1.53	20	20.6	2.58
3	18	5.3	1.2	18	5	0.32	17	5.4	1.42	1	1.7	0.45	26	28.4	2.43
1+2	31	13.3	0.33	31	8	0.55	17	19.8	2.61	19	21.4	1.02	27	37	2
1+3	32	12.7	0.33	32	7.8	0.49	18	19.4	2.2	9	23.3	0.47	33	29	2
2+3	35	7.3	0.33	35	4.75	0.48	33	16.7	2.55	12	14.8	1.32	46	34	2
1+2+3	49	13.3	0.33	49	8.6	0.56	34	19.4	2.66	20	21.3	0.75	53	37.6	1.7
r		0.79			0.71			0.49			0.77			0.8	
P		0.02			0.04			0.13			0.02			0.02	

Mean spike numbers (APs) ± 1 S.E. (SE) in response to stimulation of different numbers of aesthetascs (Aes) occurring within single zones or zonal combinations in five preparations, identified by bold-numbered dates above the columns, in addition to those graphed in Figure 7. Pearson's *r* values were obtained by linear regression analysis. Values of *P* were calculated using P-value Calculator for Correlation Coefficients, ver. 3.0 (Soper, 2014).

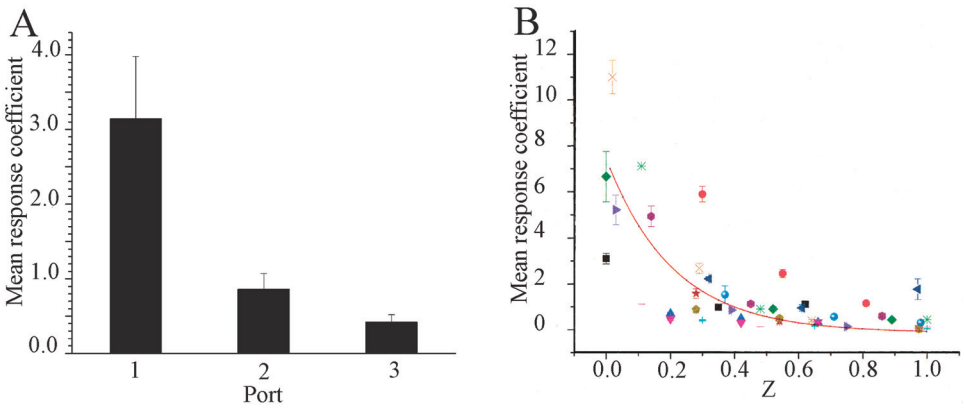

Figure 7. (A) Mean response coefficients obtained from Type I local olfactory interneurons in 14 preparations to separate stimulation *via* the three stimulus ports. Zone one, nearest the proximal origin of the aesthetasc array, consistently elicited the most vigorous responses to standard odorant exposures. (B) Graph of response coefficients in local olfactory interneurons from the same 14 different preparations against *Z,* a dimensionless variable that varies between 0 and 1 as a function of distance along the aesthetasc array from its origin to its termination at the flagellum tip. Responses from each preparation are represented here by a different colored symbol; data points in most cases are the mean of 5–10 stimulus trials ± 1 S.E. The data are satisfactorily fit by a first-order exponential decay curve defined by the equation $Y = 6.67e^{-X/.21} + 0.27$. Nonlinear regression analysis on this functional model yielded $r^2 = 0.6$ and $P < 0.0001$.

identifiable glomerulus, where synaptic connections are made with local interneurons, such as the Type I studied here, and with projection neurons to higher brain centers. In support of this putative axonal distribution pattern, uptake of radioactive tracer by ORN axons from a single pair of aesthetascs appears to be universally distributed to all ipsilateral OL glomeruli (Mellon and Munger, 1990). This distribution pattern of ORNs and their target central neurons resembles similar patterns in vertebrates, where ORNs target mitral cells that project to higher brain levels from the olfactory bulb and whose activity within the bulb is modulated by local interneurons, such as periglomerular neurons (Hildebrand and Shepherd, 1997).

Spatial summation refers to the increment in postsynaptic response in consequence of the simultaneous input from several spatially separated afferent pathways (*e.g.,* Sherrington, 1925; Eccles, 1957). Because there is presumptive evidence from recordings of local interneurons within the OL of both crayfishes (Mellon and Alones, 1995) and spiny lobsters (Schmidt and Ache, 1996), the multiglomerular distribution of these cells and their response to complex odorants indicate that they receive inputs from different classes of ORNs, thereby satisfying the criterion of excitation *via* spatially different afferent pathways. The present studies with *Procambarus* extend this concept to include different groups of similar ORNs that are spatially distributed linearly within different aesthetascs along the antennular flagellar axis. The data presented in this paper suggest, however, that considerable functional disparity exists along the linear array of aesthetascs sensilla, and their respective ORN complements, in the stimulation of olfactory deutocerebral interneurons. Our results indicate that only about the most proximal 40% of ORNs in the crayfish, *ca.* 10^4 in a large animal, are providing optimal excitation to the neurons within the deutocerebrum, and those ORNs within aesthetascs very close to the start of the array are dramatically the most effective. Port 1 was upstream of the majority of the sensillar array, however, and this raises concerns that the robust responses generated by stimulus pulses at this location are due to stimulus escape downstream to regions of the flagellum more densely occupied by aesthetascs. We ran controlled studies to test whether the presumed extent of zonal odorant exposure was, in fact, confined to its appropriate spatial location. Direct observations using planar laser-induced fluorescence (PLIF) indicate that the odorant exposures within the respective zones along the aesthetasc array were indeed confined to the localized flagellar sites. Furthermore, switching the three respective odorant supplies and removal plumbing to different ports did not have any obvious effect upon the relative effectiveness of the zonal sites in activating the deutocerebral neurons. Nonetheless, questions remain about the accuracy of odorant delivery to the circumscribed zonal regions at the three stimulus ports. Escape of some odorant from port 1 during the 0.5-s stimulus port may have spread downstream but would have been continuously diluted, encountering at its most concentrated condition a relatively low density (1–2 per annulus) of aesthetascs. The situation is very different at ports 2 and 3, however, where the annuli individually harbor more aesthetascs (4–5 per annulus), and because the annuli are smaller, where more individual aesthetascs might be exposed to stimulus escape from the local port. This means that at ports 2 and 3, in addition to the stimulus ports exposing more aesthetascs to odorant, stimulus escape, if it

occurs, would have far greater consequences in supplementing response magnitudes. Instead, the opposite appears to be true, since the response to standard stimulus pulses at these two ports was consistently, and often dramatically, less than it was at port 1. Therefore, neither PLIF experimental nor numerical considerations support the possibility that stimulus escape significantly contributed to or was responsible for the differences in stimulus efficacy at the three ports along the antennule. We conclude, therefore, that the discrepancies in response efficacy are real and must be based upon differences in the number or properties of the ORNs associated with each stimulus site or their respective central connections. A number of functional parameters could account for this. For example, disparities in the diameters or functional properties of ORN axons associated with the more distal aesthetascs would reduce the temporal density of arriving stimulus-induced action potentials at their central targets, compromising the rate of rise and/or amplitude of the resulting postsynaptic potentials. By comparison, nascent ORNs near the proximal origin of the aesthetasc array may have more uniform diameters, allowing their respective action potentials to present a more coherent temporal front at the central targets. Alternatively, ORNs associated with more distal aesthetascs may be functionally compromised by their age. In the crayfish *Cherax destructor,* it has been shown that the distal aesthetascs are the oldest on the adult flagellum, and even as new sensilla are being born at the proximal end of the array, those at the distal end are discarded with each molt as the 6–10 most distal annuli are shed (Sandeman *et al.,* 1996), as also happens in spiny lobsters (Derby *et al.,* 2003). Just as in humans and other mammals, there is a periodic turnover of ORNs. It is currently unknown, however, whether existing ORNs that are not shed are replaced at each molt cycle.

Another possible underlying cause of the disparity in sensillar efficacy is that synaptic connectivity by older, more distal ORN axon terminals within the OL may have different strengths or may be compromised through competition with terminals from nascent ORNs, especially if there are finite numbers of sites for synaptic contacts within the OLs. Although the size of the OLs and the numbers of local deutocerebral interneurons and projection neurons do increase in older crayfishes (Schmidt and Mellon, 2010; Sandeman *et al.,* 2011), the overall number of aesthetascs and their associated ORNs also increases modestly with age despite periodic shedding of the distal annuli; this raises the possibility that synaptic competition is an ongoing feature of the olfactory pathway. Finally, whatever the cellular basis for the apparent loss in individual functional competence that occurs in the ORNs associated with the more distal aesthetascs, the effect may be somewhat offset by the continued addition of more aesthetascs in the older annuli of the antennule. Even if fewer ORNs within the aging, existing aesthetascs contribute to the detection of odorants, the continual emergence of additional aesthetascs and their complement of nascent ORNs in more distal segments may act as a limited compensatory mechanism as they gradually migrate into the distal half of the array.

Acknowledgments

The research conducted in this study was supported by a grant from the National Science Foundation (CBET-0933034).

Literature Cited

Boehkoff, I., W. C. Michel, H. Breer, and B. W. Ache. 1994. Single odors differentially stimulate dual second messenger pathways in lobster olfactory receptor cells. *J. Neurosci.* **14:** 3304–3309.

Buck, L., and R. Axel. 1991. A novel multigene family may encode odorant receptors: a molecular basis for odor recognition. *Cell* **65:** 175–187.

Derby, C. D., H. S. Cate, P. Steullet, and P. J. Harrison. 2003. Comparison of turnover in the olfactory organ of early juvenile stage and adult Caribbean spiny lobsters. *Arthropod Struct. Dev.* **31:** 297–311.

Dynes, J. L., and J. Ngai. 1998. Pathfinding of olfactory neuron axons to stereotyped glomerular targets revealed by dynamic imaging in living zebrafish embryos. *Neuron* **20:** 1081–1091.

Eccles, J. C. 1957. *The Physiology of Nerve Cells.* Johns Hopkins Press. Baltimore.

Elmore, T., R. Ignell, J. R. Carlson, and D. P. Smith. 2003. Targeted mutation of a *Drosophila* odor receptor defines receptor requirement in a novel class of sensillum. *J. Neurosci.* **23:** 9906–9912.

Goldman A. L., W. Van der Goes van Naters, D. Lessing, C. G. Warr, and J. R. Carlson. 2005. Coexpression of two functional odor receptors in one neuron. *Neuron* **45:** 661–666.

Grünert, U., and B. W. Ache. 1988. Ultrastructure of the aesthetasc (olfactory) sensilla of the spiny lobster *Panulirus argus. Cell Tissue Res.* **251:** 95–103.

Hallberg, E., K. U. I. Johansson, and R. Elofsson. 1992. The aesthetasc concept: Structural variations of putative olfactory receptor cell complexes in crustacea. *Microsc. Res. Tech.* **22:** 325–335.

Hallem, E. A., M. G. Ho., and J. R. Carlson. 2004. The molecular basis of odor coding in the *Drosophila* antenna. *Cell* **117:** 965–979.

Hildebrand, J. G., and G. M. Shepherd. 1997. Mechanisms of olfactory discrimination: converging evidence for common principles across phyla. *Annu. Rev. Neurosci.* **20:** 595–631.

Mellon, DeF. 2005. Integration of hydrodynamic and odorant inputs by local interneurons of the crayfish deutocerebrum. *J. Exp. Biol.* **208:** 3711–3720.

Mellon, DeF. 2012. Smelling, feeling, tasting, and touching: Behavioral and neural integration of chemo- and mechanosensory inputs in the crayfish. *J. Exp. Biol.* **215:** 2163–2172.

Mellon, DeF., and V. Alones. 1995. Identification of three classes of multiglomerular, broad-spectrum neurons in the crayfish olfactory midbrain by correlated patterns of electrical activity and dendritic arborization. *J. Comp. Physiol.* A **177:** 55–71.

Mellon, DeF., and S. D. Munger. 1990. Nontopographic projection of olfactory sensory neurons in the crayfish brain. *J. Comp. Neurol.* **296:** 253–262.

Mellon, DeF., H. R. Tuten, and J. Redick. 1989. Distribution of radioactive leucine following uptake by olfactory sensory neurons in normal and heteromorphic crayfish antennules. *J. Comp. Neurol.* **280:** 645–662.

Mombaerts, P., F. Wang, C. Dulac, S. K. Chao, A. Nemes, M. Mendelsohn, J. Edmondson, and R. Axel. 1996. Visualizing an olfactory sensory map. *Cell* **87:** 675–686.

Ressler, K. J., S. L. Sullivan, and L. B. Buck. 1993. A zonal organization of odorant receptor gene expression in the olfactory epithelium. *Cell* **73:** 597–609.

Sandeman, D. C., and J. Denberg. 1976. The central projection of chemoreceptor axons in the crayfish revealed by axoplasmic transport. *Brain Res.* **115:** 492–496.

Sandeman, D. C., F. Bazin, and B. S. Beltz. 2011. Adult neurogenesis: examples from the decapod crustaceans and comparisons with mammals. *Arthropod Struct. Dev.* **40:** 258–275.

Sandeman, R. E., and D. C. Sandeman. 1996. Pre- and postembryonic development, growth, and turnover of olfactory receptor neurons in crayfish antennules. *J. Exp. Biol.* **199:** 2409–2418.

Schmidt, M., and B. W. Ache. 1996. Processing of antennular input in the brain of the spiny lobster, *Panulirus argus.* II. The olfactory pathway. *J. Comp. Physiol.* **178:** 605628.

Schmidt, M., and DeF. Mellon. 2010. Neuronal processing of chemical information in crustaceans. Pp. 123 –147 in *Chemical Communication in Crustaceans,* T. Breithaupt and M. Thiel, eds. Springer. New York.

Sherrington, C. S. 1925. Remarks on some aspects of reflex inhibition. *Proc. R. Soc. B* **97:** 519–545.

Soper, D. 2014. Statistics calculators: p-value calculator for correlation coefficients. [Online]. Available: http://www.danielsoper.com/statcalc3/calc.aspx/id=44 [2014, 28 July].

Tierney, A. J., C. S. Thompson, and D. W. Dunham. 1986. Fine structure of aesthetasc chemoreceptors in the crayfish *Orconectes propinquus. Can. J. Zool.* **64:** 392–399.

Vosshall, L. B., H. Amrein, P. S. Morozov, A. Rzhetsky, and R. Axel. 1999. A spatial map of olfactory receptor expression in the *Drosophila* antenna. *Cell* **96:** 725–736.

Vosshall, L. B., A. M. Wong, and R. Axel. 2000. An olfactory sensory map in the fly brain. *Cell* **102:** 147–159.

Zhang, X., and S. Firestein. 2002. The olfactory receptor gene superfamily of the mouse. *Nat. Neurosci.* **5:** 124–133.

Zou, Z., L. F. Horowitz, J. P. Monmayeur, S. Snapper, and L. B. Buck. 2001. Genetic tracing reveals a stereotyped sensory map in the olfactory cortex. *Nature* **414:** 173–179.

Zufall, F., S. Firestein, and G. M. Shepherd. 1994. Cyclic nucleotide-gated ion channels and sensory transduction in olfactory receptor neurons. *Annu. Rev. Biophys. Biomol. Struct.* **23:** 577–607